


Cite this: *RSC Adv.*, 2021, **11**, 23644

Received 2nd April 2021  
Accepted 18th June 2021

DOI: 10.1039/d1ra02611a  
rsc.li/rsc-advances

## Lignin biopolymer: the material of choice for advanced lithium-based batteries

Marya Baloch and Jalel Labidi \*

Lignin, an aromatic polymer, offers interesting electroactive redox properties and abundant active functional groups. Due to its quinone functionality, it fulfils the requirement of erratic electrical energy storage by only providing adequate charge density. Research on the use of lignin as a renewable material in energy storage applications has been published in the form of reviews and scientific articles. Lignin has been used as a binder, polymer electrolyte and an electrode material, *i.e.* organic composite electrodes/hybrid lignin-polymer combination in different battery systems depending on the principal charge of quinone and hydroquinone. Furthermore, lignin-derived carbons have gained much popularity. The aim of this review is to depict the meticulous follow-ups of the vital challenges and progress linked to lignin usage in different lithium-based conventional and next-generation batteries as a valuable, ecological and low-cost material. The key factor of this new finding is to open a new path towards sustainable and renewable future lithium-based batteries for practical/industrial applications.

### 1. Introduction

The fundamental challenges for the future progress and wide-ranging use of electrochemical energy storage systems (EESs) are a better performance and safety measurements including the production and material costs, the implementation of environmentally friendly materials and manufacturing processes, as well as developing easy recyclability and up-

scalability.<sup>1,2</sup> However, EES devices run on the basis of inorganic and/or rare metal electrodes (Mn, Co, Ni and Fe), polymeric binders (such as PVDF mixed with toxic NMP solvents), and volatile non-aqueous electrolytes (organic carbonates such as DMC and DEC, or ethers such as DME and DIOX), which are fundamentally expensive and toxic with imperishable impacts on the environment.<sup>3-6</sup> However, it is possible to replace them with a low-cost and non-toxic material that could provide properties and

Department of Chemical and Environmental Engineering, School of Engineering, Donostia-San Sebastian, Gipuzkoa, Spain. E-mail: [jalel.labidi@ehu.es](mailto:jalel.labidi@ehu.es)



*Marya Baloch obtained her PhD in lithium-sulphur batteries within Inorganic chemistry from CIC-Energigune, Miñano in 2016. Currently, she is a researcher at the University of the Basque Country (UPV/EHU), Spain, where she works in the Biorefinery Processes (BioRP) research group within the Department of Chemical and Environmental Engineering under the direction of Jalel Labidi. Her research work focuses on the improvement of electrochemical properties of materials derived from renewable resources such as biomass materials, where she seeks the fundamental understanding of biomass-derived polymers conversion into a functional battery material.*



*Jalel Labidi obtained his PhD in Chemical Engineering from Institut National Polytechnique de Lorraine – INPL – Nancy, France, in 1992. He is presently senior research scientist at the University of the Basque Country (UPV/EHU), Spain, where he teaches courses at the master level. His main fields of interest and expertise are biomass transformation into commodity chemicals and polymers, biomaterials, separation processes and chemical process design.*



features that an EES technology demands. Organic compounds as battery components have gained much interest from scientific communities, due to their fast reaction kinetics and high rate capability;<sup>7</sup> they could be a perfect match for high power energy storage applications. Naturally, organic materials show poor ionic and electrical conductivity that could critically hinder their credibility as a high-performance energy source.<sup>8</sup> Thus, a natural abundant material that offers an electroactive redox reversible reaction and capacity that mitigates these drawbacks can be the material of choice leading the battery technology to be a promising candidate for an efficient, cheap and longer lifetime EESs.<sup>4</sup>

Lignin, a biomass-derived organic polymer and a major by-product of the paper industry, is a carbonyl compound with quinone functionality that fulfils the requirement of a cheap and abundant material for erratic electrical energy storage by only providing suitable charge density.<sup>9</sup> It offers a versatile chemical structure and functional groups, which can lead towards advanced molecular tailoring modifications suitable for the application. Lignin has been used for decades as a cheap carbon source within the industrial-level production processes.

The major aim of this review is to emphasize the use of lignin as an improvised battery material in accessible available lithium battery systems. However, there have been few reviews explaining the application of lignocellulosic biomass as an active component in different EESs;<sup>10–15</sup> but, our focus is mainly on up-to-date advances related to the electrochemical performance of lignin in Li-based systems as an active electrode (cathode/anode), binder, electrolyte and a major carbon source. This review mainly attributes lignin as a replacement to well-known frequently used expensive and harsh battery materials. This is a meticulous follow-up of the role of lignin with respect to its functionality showing the evolving interest in biomass-derived lignin biopolymers.

### 1.1 Lignin, its functionality and redox activity

Lignin is a phenolic biopolymer that is produced in larger quantity of ~50 000 000 tons each year, and due to its aromatic and inhomogeneous complex chemical structure, it is habitually used for combustion of pulps and paper industry boilers.<sup>16–19</sup> Traditionally, 15–33 wt% of lignin contents are present in any biomass;<sup>20,21</sup> Table 1 shows the percentage of lignin in basic wood types. Usually, lignin is based on three aromatic alcohols, sinapyl, coniferyl, and *p*-coumaryl, as shown in Fig. 1, and their production is essentially depending on the position of methoxy group attachment on the phenol group of the lignin. These alcohols further produce monolignols, *i.e.* syringyl (S), guaiacyl (G) and *p*-hydroxyphenyl (H). Lignin as an amorphous polymer network differs in functionalities due to its original plant type, extraction methods and experimental conditions.<sup>22,23</sup>

Table 1 Percentage (dry) of lignin usually found in softwood, hardwood and annual plant wood types

Wood type	Plant	Lignin%	Ref.
Softwood	Pinewood	34.4 ± 0.3	57
Hardwood	Eucalyptus	25.2 ± 1.1	58
Annual plant	Grass	11.55 ± 0.3	59

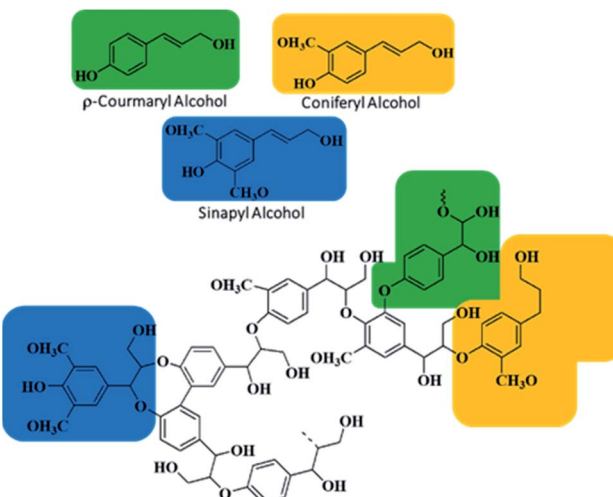


Fig. 1 Chemical structure of the lignin molecule showing three alcoholic monolignols, *p*-coumaryl, coniferyl, and sinapyl.

The complex heterogeneous chemical structure of lignin offers unique functionalities such as methoxy groups, hydroxyl (aliphatic and aromatic) groups, carbonyl (C=O) groups, carboxyl groups and a large number of aromatic rings<sup>24</sup> ready to be harnessed for their potential chemical functions, that lead further to production of chemicals and allows a vast number of chemical modifications for various applications, for instance, the –OH group of lignin can further result in a wide range of polymeric compounds, higher carbon content (~60%, due to generous amount of C=O functionalities), bio-degradability, antimicrobial behaviour, adhesive properties, eminent thermal stability, and relative abundance. It also shows additive properties, dust dispersant and blending properties.<sup>19,25</sup> The irregular complex molecular structure of lignin with a highly condensed linkage provides higher mechanical strength and rigidity to resist exterior forces.<sup>18–20</sup> In general, the behaviour of lignin is basically dependent on these functional groups and their positions. However, the understanding of lignin's chemical structure is rather complicated due to its 3D irregular network order. The nature and valorisation of lignin has been thoroughly discussed in assorted publications and reviews over the years.<sup>26–35</sup>

The interesting functional group for the application of energy storage is the quinone moiety of the lignin, and quinones are basically dyes in plants, whereas it can facilitate a fast and reversible two electron/proton redox reaction, thanks to its six-membered ring with C=O functional group staging anthracene, benzene and naphthalene chains.<sup>36–38</sup> This property can be sufficiently explored to present lignin as a bio-based energy conversion material. The oxidation of methoxy groups S and G monolignols activates quinone species (quinone and derivatives like hydroquinone), and the charge transfer reaction of quinone/hydroquinone has been noted upon repeated cycling within the electrolyte between the electrodes.<sup>39–42</sup> However, it has been stated that in order to allow charge storage, a conductive additional component is needed to share the responsibility of providing electronic conductivity and electroactive redox activity.<sup>43,44</sup>



## 1.2 Lignin and quinone functionalities in energy storage systems

The investigation on lignin in the field of energy storage systems is indispensable, due to the fact that the research studies so far on the electrochemical/electrical behaviour of pure lignin are rather scarce. Meanwhile, lignins, due to their diverse functionalities, can play different roles in ESSs, for example, lignosulfonate (LS) can provide sulphur doping agents in EES devices<sup>45,46</sup> and alkali lignin proves itself to be quite useful for the application of building nanomaterials *via* electrospinning.<sup>47</sup> Hydrolysed lignin has been used as a cathode,<sup>48</sup> organosolv lignin and acetone lignin as anodes,<sup>49,50</sup> Kraft lignin as a binder and a cathode<sup>51,52</sup> and most of the lignins are widely used as carbon precursors.<sup>50,53-56</sup>

Nonetheless, lignin has always been forecasted as an insulating material as other organic compounds, where prevailing sufficient electrochemical redox activity could be quite challenging.<sup>23</sup> However, several studies provide the subsequent proof of reversible potential cycling and faster electron transfer kinetics of active redox of the quinone groups, which perceptibly is derived from electro-oxidation of lignins.

Quinone functional groups are mainly responsible for the redox activity of biopolymer materials *via* electron exchange. They consist of a conjugated cyclic structure with two ketone groups, where under redox reactions, the conjugated double bond undergoes cleavage/formation influencing the performance of the electrochemical battery.<sup>60-62</sup> High content of quinone groups can be easily achieved by oxidation of the phenolic groups of lignin, which controls the redox activity of most quinones such as anthraquinone and naphthaquinones, due to their property of undergoing a  $2e^{-}/H^{+}$  reversible redox transfer at low potential.<sup>63,64</sup> The biggest issue with the usage of quinone biopolymers as a battery material is their solubility in the electrolyte solvents resulting in poor cycling life and performance. Research focused on this particular problem is crucial, and various methods have been applied to reduce the dissolution of organic electrode materials, for example, grafting onto the solid substrate to avoid mobilization within the electrolyte, but this affects the specific capacity of the battery. Polymerization of the organic material into a high-molecular weight polymer can help with the solubility issue, but again this affects the energy density negatively. The possible solution could also be providing an intermediate to help both cycling life and energy density. However, it has been proven that quinone functionalities perform best upon hybridization with a conductive material (organic or inorganic) for the energy storage applications.<sup>65-69</sup>

Lignin mixed with synthetic or bio-polymers can show promising properties such as the antioxidant property of the phenolic groups providing better resistance to oxidative degradation. However, to further exploit the properties of lignin, chemical modifications will be required. It is promising to use the lignin directly derived from biomass, but to allow charge storage/transfer, a hybrid material (synthetic or bio-polymer) is needed, where one component provides electronic conductivity and the other redox reactivity, respectively.<sup>43</sup> When mixed with polyaniline, lignin represents two redox peaks around 0.7 and 0.9 V. The interaction of kraft lignin from *Eucalyptus grandis* with polyaniline was confirmed by an FTIR peak at  $1146\text{ cm}^{-1}$  of the

protonated amine vibration band. The value of electrical conductivity was totally dependent on the homogenous mixture of the PANI/lignin blends, and SEM shows the homogenous nature of the films without agglomeration of the globules of lignin, proving the miscibility of two polymers<sup>70</sup> that could demonstrate the adoptability of lignin with synthetic polymers upon mixing.

Naturally derived lignin hybrid composites could provide sufficient charge transfer due to faradic processes of lignin activated *via* repeated electrochemical redox cycling. The hybrid composite of the LS lignin with polypyrrole (PPY/LS), where polypyrrole was electro-polymerised in the presence of lignin dopants, improves the charge storage ability of the hybrid composite electrode. The process was confirmed by *in situ* FTIR spectroscopy, giving a significantly visible IR band of quinone at  $\sim 1705\text{ cm}^{-1}$  and hydroquinone at  $\sim 1045\text{ cm}^{-1}$ . The reversible redox reaction was confirmed by the vibrations bands of C=O and C-O at  $1706$  and  $1043\text{ cm}^{-1}$ , respectively. This hybrid mixture of polypyrrole and the LS lignin electrode shows a discharge capacity of  $72\text{ mA h g}^{-1}$  that is higher than that of the pure polypyrrole electrode ( $30\text{ mA h g}^{-1}$ ). Nonetheless, the cycling stability of this PPY/LS hybrid material electrode is poor with a dramatic loss of quinone redox capacity after 1000 cycles.<sup>72</sup> It might be due to overconsumption/over oxidation of guaiacyl's quinone functionality, where possible covalent bonds cleave and facilitate a nucleophilic attack over quinone moieties, leading to poor performance of the PPY/LS hybrid composite.<sup>72</sup>

Subsequently, 3,4-ethylenedioxythiophene (EDOT) is applied to obtain the PEDOT/LS hybrid material electrode, which displays a much better cycling stability with 83% capacity retention after 1000 charge-discharge cycles and a discharge capacity of  $34\text{ mA h g}^{-1}$ , with 140% capacity increase compared with PEDOT ( $14\text{ mA h g}^{-1}$ ).<sup>73</sup> It has been established that to boost the performance of lignin in an electrochemical system, the contribution of the hybrid material's ionic and electronic charge transfer abilities is crucial.<sup>74</sup>

The carbonyl functional groups present in organic compounds could be a source for higher theoretical capacity,<sup>75</sup> but added C=O groups might lack in active sites upon incorporation into the larger coordinated units, leading to a lower practical capacity.<sup>76,77</sup> The units of *p*-quinone are used for they can provide sufficient active sites due to macrocyclic molecular structures and aid to achieve high efficiency.<sup>78,79</sup> The macrocycle pillar[5]quinone (P5Q) has five methylene bridges linking quinone groups at the *para* position, and it undergoes oxidation process similarly to the quinone group<sup>39-41</sup> of lignin to activate the charge transfer process within the electrolyte and electrode, as shown in Fig. 2a. It was cycled in an all-solid-state lithium organic battery to generate repeating 1,4-benzoquinone units, leading to the resulting final product that could intercalate  $\sim 10$  Li<sup>+</sup> ions providing a high specific capacity of  $418\text{ mA h g}^{-1}$ , thanks to its active carbonyl sites (Fig. 2b).<sup>71</sup>

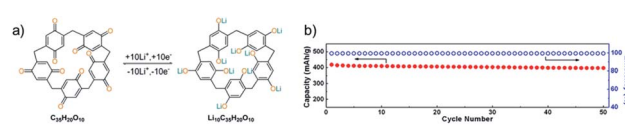


Fig. 2 (a) Mechanism of electrochemical redox activity of P5Q. (b) All-solid-state lithium organic battery capacity and coulombic efficiency.<sup>71</sup>



The electrochemistry of modified lignin *via* electrochemical polymerization in thin layers was tested by electrocatalysis,<sup>39,41</sup> proving the hypothesis that if lignin is mixed well with sufficiently good electronic/ionic conductive materials, it could permit charge transference back and forth from a quinone site using redox reactions.<sup>40,80,81</sup>

Phenol-formaldehyde condensation of homopolymers and copolymers of syringol (S) and guaiacol (G) leads to the polymerization of a well-defined synthetic model compound of lignin for the purpose to mimic the hardwood and softwood lignin conduct. The models were prepared to obtain a precise chemical structure with controlled phenol reactivity and purity for a well-defined hybrid composite as a final product, *i.e.* by incorporating synthetic lignin into single-wall carbon nanotubes (SWNTs) and polypyrrole (PPy) electron-conducting matrixes, whereas hydroquinone was used to augment the quinone functionalities to direct towards enhanced charge capacity (max. capacity 94 mA h g<sup>-1</sup>). It was demonstrated that well-defined synthetic lignin provides an efficient electronic transference due to the presence of hydroquinone, which helps reducing the amount of additional conductive materials (only 20 wt% of SWNTs).<sup>44</sup>

## 2. Lignin in lithium batteries

The possibility of lignin as an alternative battery component has already been explored in many rechargeable electrochemical systems, where lignin has played a significant role as a cathode, binder, electrolyte, and anode. Herein, we briefly summarise the use of lignin in different battery technologies in different manners.<sup>82,83</sup>

Up to now, the major application of lignin in the EES was as a cheap carbon precursor, and lignin carbon proves to be an attractive choice due to its reduced energy consumption, cost and minimum CO<sub>2</sub> emission, thus, it can be considered as a replacement for popular polyacrylonitrile (PAN ~13 € per lb)-based carbons that require high treatment temperatures ( $\leq 1000$  °C to  $\geq 2000$  °C), which could be a virulent process for the environment. Lignin has the vantage ample carbon content due to the C=O functionality. Similarly, the highly rich aromatic structure of lignin allows a great deal in tuning the morphology of carbon, resulting in different forms, although the resulting shape is primarily influenced by the origin of lignin.<sup>84-86</sup>

Extensive research has been carried out on lignin-derived carbons in the course of patents and reports since the 1960s. Lignin-based carbon materials have drawn much attention due to their use as anodes or as active carbon electrode materials<sup>12,51,87</sup> in lithium/sodium-ion batteries<sup>85,88,89</sup> and supercapacitors.<sup>87,90,91</sup>

Due to diverse heterogeneous morphology of lignin, the diffusion of lithium (Li<sup>+</sup>) ions is much easier leading it to be a low-cost electrode material in primary and rechargeable lithium batteries. Simultaneously, the distinctive lignin functional groups (C=O, OH, C-O-C) show strong electroactive redox properties towards Li<sup>+</sup> ions. Owing to that, a primary Li/lignin cell could achieve the maximum capacity of ~600 mA h g<sup>-1</sup>. Heretofore, this review presents a brief summary of lignin use in diverse Li-based systems.

### 2.1 Primary lithium batteries

Hydrolysed lignin as a cathode in primary lithium batteries shows a discharge capacity of 445 mA h g<sup>-1</sup> due to the interaction of lithium ions with the ether group; however, its double the amount of specific capacity expected probably due to the presence of carbon black. Voltage plateaus at ~1.8 and ~1.1 V indicate the step-by-step discharge character of electrochemical reactions of lithium ions with oxygen of different characteristic groups present in the lignin characterized by XPS and IR.<sup>48</sup> The incurred results conclude HL as a validated cathode material due to its low cost as compared to other available primary lithium batteries, whereas the Klason lignin (KL) cathode shows a specific capacity of 380 mA h g<sup>-1</sup> for sun flower-derived lignin (SFDL) and 600 mA h g<sup>-1</sup> for buckwheat-derived lignin (BWDL).<sup>23,92</sup> The SEM study depicts that each lignin type has a different surface morphology, which seems to ease the Li<sup>+</sup> ion diffusion within lignin particles, whereas EDS gave an estimate of oxygen content, *i.e.* SF-KL, BW-KL and HL contains 40, 35 and 23 wt% of oxygen, respectively. The presence and interaction of these oxygen groups help to allow the practical discharge capacity of 450 mA h g<sup>-1</sup> *versus* Li-anodes.<sup>48</sup>

### 2.2 Lithium-ion batteries (LiBs)

Li-ion batteries (LiBs) are the most promising candidate of the EES for large-scale applications such as electric vehicles (EVs) and major electronic devices. The conventional lithium ion battery is composed of three basic components: the anode usually carbon, *i.e.* graphite, *etc.*, the cathode is mainly a metal oxide with polyanion containing lithium and electrolyte an organic solvent containing lithium salts. This facilitates the redox reaction/transference of Li<sup>+</sup> ions back and forth between the anode and the cathode (Fig. 3).<sup>93</sup>

LiBs can be the solution to some of our society's most pressing challenges such as high CO<sub>2</sub> emission from the transport industry, energy poverty and as a green alternative to store renewable energy. However, Li-ion batteries are too expensive, and the most challenging problem in LiBs is the safety issue, beside the environmental effects of detrimental battery components. Thus, the replacement of these materials with bio-polymers like lignin can be a solution.

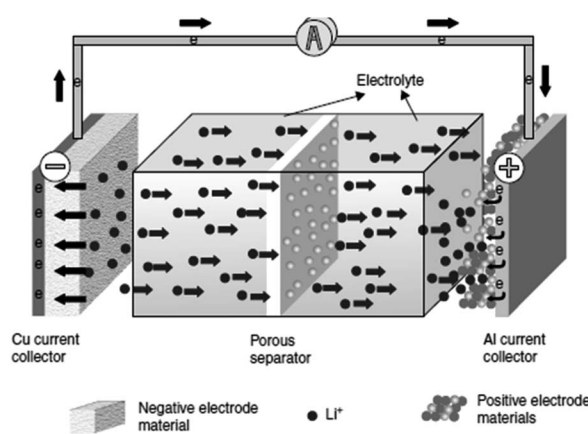


Fig. 3 Working mechanism of a conventional Li-ion battery.<sup>93</sup>



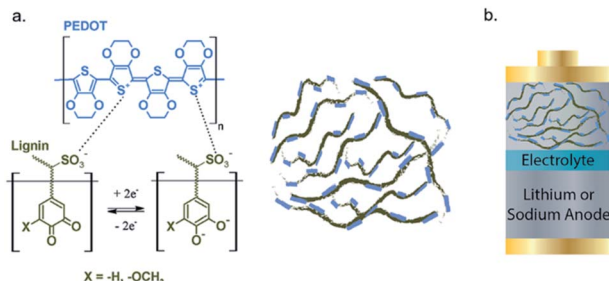


Fig. 4 (a) Structural representation of lignin, PEDOT, and (b) assembled Li/PEDOT hybrid as cathode in the  $\text{Li}^+/\text{Na}^+$ -ion battery. Reproduced from ref. 94 with permission from The Royal Society of Chemistry.

However, lignin has been used as an active electrode, binder and as an electrolyte, but it has gained much popularity as a hybrid composite, where a conductive polymer is mixed with a lignin biopolymer to attain the desired electroactive properties and coupled redox progressions.

The combination of 20% insulating lignin in bulk amount (80%) of conductive PEDOT (poly(3,4-ethylenedioxythiophene)) can improve the electronic conductivity and transport of lignin. The lignin/PEDOT hybrid composite, as shown in Fig. 4, was analysed in Li-ion batteries and the maximum delivered capacity of  $\sim 50 \text{ mA h g}^{-1}$  at C/20 cycling rate in  $\text{LiPF}_6$  and  $\text{NaPF}_6$  was achieved, higher than the capacity of lignin and PEDOT, individually. Furthermore, conductive carbon was added into the mixture of lignin/PEDOT to further increase the  $\text{Li}^+$  ion diffusion and electronic conductivity, and the capacity was increased up to  $159 \text{ mA h g}^{-1}$ .<sup>94</sup>

Carbon-anodes have been extensively used in LIBs and their demand has increased within time owing to their facile  $\text{Li}^+$  ion intercalation, existence in larger quantity with cheap prices and their high chemical stability. As established, lignin is one of the auspicious applicant for carbon production, though, mixing carbon with lignin itself can provide a hybrid L-C composite with enhanced reversible  $\text{Li}^+$  capacity and faster kinetics. The faradic and non-faradic charge storage studies of a hybrid composite of conductive carbon with commercially available unmodified kraft lignin displays a capacity of  $80 \text{ mA h g}^{-1}$ , where the charge storage of conductive carbon has been boosted by the contribution of the additional redox chemical activity of lignin.<sup>51</sup>

Lignin has also been used to reduce the decomposition of electrolyte and help to increase the battery lifetime with a major -OH (phenolic) group, which behaves as a free radical scavenger. It has been proven quite beneficial in LIBs, where

carbonate-based electrolytes are used, and they experience solvent polymerization and create cathode/electrolyte interphase (CES), due to alkyl free radicals decomposed through oxidation when the voltage exceeds 4.3 V. The organic liquid electrolytes in LIBs face a grave safety issue including fire hazard, leakage, and worst case scenario a blast. Therefore, gel polymer electrolytes (GPEs) gained quite a lot of popularity because of limited liquid presence within the electrolyte; however, some GPEs are not easily biodegradable such as polyacrylonitrile (PAN), polyvinyl acetate (PVA), polyvinylidene fluoride (PVDF), and polyethylene oxide (PEO). The continuous usage of GPEs in LIBs will result in a grand disaster "white pollution" in the natural environment; thence, lignin as an ample natural biopolymer could be a great replacement of synthetic polymer electrolytes.<sup>95</sup> Lignin-based GPE (L-GPE) membranes can uphold liquid electrolytes as high as  $\sim 230$  wt% with an exceptional ionic conductivity of  $3.73 \text{ mS cm}^{-1}$  at RT. The LGPE membrane was prepared in water and collected after simple drying, which imposed the process as green and environment friendly. Nonetheless, the LGPE membrane shows thermal stability of  $250^\circ\text{C}$  along with a higher  $\text{Li}^+$  ion transference of 0.85, thanks to the phenolic hydroxyl functional group of lignin interacting strongly with anions in lithium salts. The potential use of L-GPE could be proven by its electrochemical stability within the voltage range of 2.5–4.2 V and its good compatibility with the Li-anode during cycling. Nevertheless, the mechanical strength is poor as compared to the standard GPE membrane; to improve the mechanical strength, PVP has been introduced to compose a lignin/PVP membrane. PVP/lignin composite membrane exhibits an amended mechanical property and astonishing safety as severe requirements of LIBs. Additionally, after 100 cycles, the PVP/lignin composite Li-ion cell shows a phenomenal capacity retention of 95.3% with a capacity of  $135 \text{ mA h g}^{-1}$  at a current density of 0.2C.<sup>101</sup>

Conventional and widely used binder in LIBs, polyvinylidene fluoride (PVDF), reacts with the lithium metal anode during cycling that forms a stable  $\text{LiF}$  (lithium fluoride) compound affecting the cycling performance of the cell, while introducing lignin as a binder, in the well-known cathode ( $\text{LiFePO}_4$ ) versus graphite anode gives a comparatively high specific capacity and stability. Reversible capacities of 148 and  $305 \text{ mA h g}^{-1}$  have been shown for the lignin-bound cathode and anode at a C-rate of 0.1C, respectively. In comparison with a PVDF-bound cathode cell that shows a capacity retention of 46.2%, the lignin-bound cathode gives a capacity retention of 94.1% after 1000 cycles with a specific capacity of  $110.8 \text{ mA h g}^{-1}$  and a coulombic efficiency of 99.5%.<sup>102</sup>

Table 2 Outline of recent lignin application in Li-ion batteries

Materials	Function	Performance	Ref.
Organosolv lignin and PLA and PTU	Anode	$611 \text{ mA h g}^{-1}$ with 500 cycles	50
Lignin carbon/Si (Si@C)	Anode	$955 \text{ mA h g}^{-1}$ with 51 cycles	96
Alkali lignin (AL)/SiNPs	Anode	$882 \text{ mA h g}^{-1}$ after 150 cycles	97
Sodium lignosulfonate/NiO	Anode	$863 \text{ mA h g}^{-1}$ after 100 cycles	98
$\text{LiNi}_{0.5}\text{Mn}_{1.5}\text{O}_4$ /lignin/graphite/acetylene black	Binder	$110.8 \text{ mA h g}^{-1}$ after 1000 cycles	99
Sodium polyacrylate grafted on alkali lignin	Binder (silicone anode)	$1914 \text{ mA h g}^{-1}$ after 100 cycles	100



Table 2 shows some recent developments of lignin as an anode and binder in LIBs; however, the lignin has been complimented with an active polymeric compound to enhance the electronic conductivity and redox activity during cycling. A lignin carbon nanofiber anode was prepared by mixing with polylactic acid (PLA) and thermoplastic elastomeric polyurethane (TPU). The morphology was controlled by concordance of lignin with PLA/TPU in the mix; however, PLA introduced the porous quality to the final carbonised product. The porosity of the lignin/PLA blend helps enhancing the performance of the LIB by showing  $670 \text{ m}^2 \text{ g}^{-1}$  for a 50 : 50 ratio of lignin/PLA, whereas  $345 \text{ m}^2 \text{ g}^{-1}$  for 50 : 50 of lignin/TPU.<sup>50</sup> To improve the cycling life and performance, lignin has been pyrolysed with silicon to achieve carbon-coated silicon (Si@C), which gives a specific capacity of  $955 \text{ mA h g}^{-1}$  after 51 cycles. It shows even better results upon cycling at  $800^\circ\text{C}$  ( $1515 \text{ mA h g}^{-1}$ ).<sup>96</sup> However, using alkali lignin (AL) and its derivative azo polymer (AL-azo-NO<sub>2</sub>) to fabricate Si@C shows that upon the addition of an azo group, the anode shows better performance with increased electronic conductivity due to N-doping. It gives a specific capacity of  $882 \text{ mA h g}^{-1}$  with a coulombic efficiency of 99% at 150 cycles.<sup>97</sup> The controlled morphological hierarchical mesoporous carbon (HMPC) derived from lignosulfonate was later on incorporated into Ni(OH)<sub>2</sub> to obtain NiO-HMPC. Further, the final product was thermally annealed without having any difference in the nanosphere morphology and shows a higher surface area  $852 \text{ m}^2 \text{ g}^{-1}$  that helps Li<sup>+</sup> ion diffusion easier and exhibit a discharge capacity of  $863 \text{ mA h g}^{-1}$  at  $0.1 \text{ A g}^{-1}$  after 100 cycles.<sup>98</sup>

Similarly, the role of lignin as a binder has also been explored within the LIB cathode and anode, where it was introduced within the LiNi<sub>0.5</sub>Mn<sub>1.5</sub>O<sub>4</sub> cathode<sup>99</sup> and silicon micro particle anode as grafted on sodium polyacrylate (PAL-NaPAA),<sup>100</sup> providing stable cycling life as compared to the conventional PVDF binder. It shows a capacity of  $110.8 \text{ mA h g}^{-1}$  with 99.5% of coulombic efficiency after 1000 cycles for the LiNi<sub>0.5</sub>Mn<sub>1.5</sub>O<sub>4</sub> cathode<sup>99</sup> and the PAL-NaPAA anode shows a lithiation capacity of  $800 \text{ mA h g}^{-1}$  for over 940 cycles.<sup>100</sup> These examples anticipate the easy use of lignin within LIB systems as an active component. LIBs may be proven as the best choice for energy-related challenges, but due to high cost of cathode materials, next-generation low-cost batteries such as lithium-sulphur, lithium-oxygen and lithium-selenium batteries have been introduced. Our motive here is to give just a brief introduction of lignin usage in these beyond lithium-ion batteries.

### 2.3 Lithium-sulphur (Li-S) batteries

Li-S batteries could be an interesting choice owing to their inexpensiveness and abundance of the cathode materials. The working principle of Li-S batteries is similar to Li-ions, except that sulfur accepts  $2 \text{ Li}^+$  ions allowing a high specific capacity of  $1675 \text{ mA h g}^{-1}$ . Sulphur, like lignin, is insulating itself, thus, it is usually impregnated into conductive carbon to provide the electrical conductivity. Conductive carbon submerging with sulphur also helps restrict the polysulphide diffusion, which leads to cycling stability of Li-S batteries. Li-S battery's prime

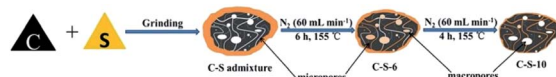


Fig. 5 Graphic representation of the encapsulation of sulphur into carbon mixtures.<sup>103</sup>

problem is shuttling of polysulphide species within the liquid electrolyte, *i.e.* usually faster active sulphur mass consumption affecting the cycling life of the battery. To systematically suppress the shuttling of the polysulphide species within the electrolyte in Li-S, the multiwall carbon nanotubes (MWCNTs) were used, which are rather expensive. In order to replace expensive conductive carbon, lignin has been used as an alternative source of carbon. It can be carbonized at high temperatures; to avoid shuttling, MWCNTs were mixed and the impacts were investigated. When 25 wt% of lignosulphonate (LS) lignin was employed in MWCNTs as a protection layer, minimum capacity decay with a higher initial discharge capacity at a cycling rate of 0.5 and 1C was observed,<sup>104</sup> whereas using LS as a binder to replace the conventional PVDF binder that cannot mitigate the shuttling effect leading to low electrochemical performance, a higher specific discharge capacity of  $\sim 1307 \text{ mA h g}^{-1}$  at a cycling rate of 0.1C was achieved in comparison to PVDF ( $706 \text{ mA h g}^{-1}$ ) with a capacity retention of 71.9%.<sup>105</sup>

Nonetheless, the encapsulation of sulphur within the micro-porous carbon network derived from commercially available lignin (Fig. 5) allows high surface area, reasonable pore size, and the outer surface to pretend as a functionalised matrix, due to the presence of oxygen functional groups. The encapsulation was controlled by time; the samples were collected after 6 hours (C-S-6) and 10 hours (C-S-10). The results indicate that prolonged duration of impregnation leads to better battery performance due to the negative impacts of polysulphide transition in the electrolyte, perhaps, owing to the micro/macroporous network of lignin carbon. The C-S-10 shows a discharge capacity of  $1241 \text{ mA h g}^{-1}$  with a specific capacity of  $791 \text{ mA h g}^{-1}$  at 100th cycle.<sup>103</sup>

Yet, in any Li-based system, it appears that lignin can be beneficial due to the presence of its oxygen functional groups when carbonised, whereas the mixture with GPE can demonstrate an astonishing ionic conductivity of  $4.52 \text{ mS cm}^{-1}$  at RT. Lignin-GPE (L-GPE) as a separator and electrolyte in Li-S batteries shows a capacity retention of 55.1% at  $20 \text{ mA g}^{-1}$  with discharge capacity in the range from 1186.3 to  $653.5 \text{ mA h g}^{-1}$  for 100 cycles, where the liquid electrolyte cell only attained a discharge capacity of  $242.2 \text{ mA h g}^{-1}$  with low capacity retention (21.4%), confirming the hindrance of the polysulphide diffusion leading to better electrochemical performance.<sup>106</sup>

Hydrothermal carbonization of activated lignin with KOH and further doping yield nitrogen-doped nanoporous carbon with a honeycomb structure (n-hC), where sulphur was impregnated within the well-organized micro/mesoporous honeycomb structure for better electrochemical and thermal stability among redox processes, which gives an initial discharge capacity of  $\sim 1295 \text{ mA h g}^{-1}$  at 0.1C after 600 cycles.



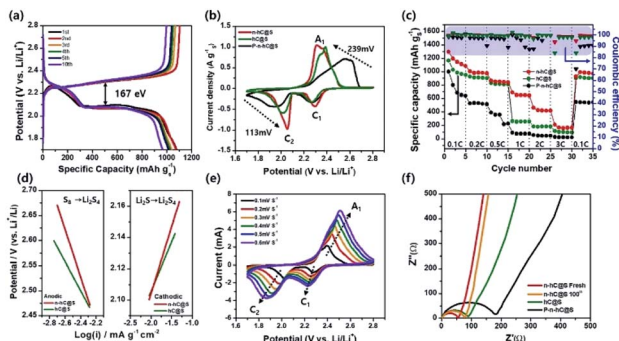


Fig. 6 (a) Sulphur-confined nitrogen-doped activated carbon composite charge and discharge plateaus. (b) Cyclic voltammograms. (c) Rate capability cycling test of sulphur-confined nitrogen-doped activated carbon, sulphur-confined honeycomb-activated carbon and polysulphide-confined nitrogen-doped honeycomb-activated carbon. (d) Tafel comparison plots. (e) CV at different scanning rates of sulphur-confined nitrogen-doped activated carbon. (f) EIS plots before and after 100 cycles of sulphur-confined nitrogen-doped activated carbon in comparison with sulphur-confined honeycomb-activated carbon and polysulphide-confined nitrogen-doped honeycomb-activated carbon.<sup>107</sup>

Thus, a well-organized hierarchical structure helps the  $\text{Li}^+$  ion diffusion and the presence of nitrogen helps the faster kinetics, as shown in Fig. 6d, Tafel plots current density exchange. Thus, it is proven that the functionalities of the lignin and rich-carbon structure play an important role in the carbon morphology that later on helps confining the highest amount of sulphur (64.1 wt%) and reversible redox reactions.<sup>107</sup> A separator plays an important role in Li–S batteries, and hence, lignin nanoparticle-coated Celgard (LC) was introduced to induce the chemical binding of polysulphide species using essential electron-donating groups and reduce the shuttling. It aids the cycling stability of the Li–S cell with a typical sulphur cathode (sulphur with acetylene black) for over 500 cycles as compared to the normal Celgard separator at 1C.<sup>108</sup>

Nonetheless, lignosulfonate sodium salt (LSS), an inexpensive biopolymer derived from the waste of wood mills was used as a binder that improved the capacity and cycling retention, due to the complex and distinctive chemical structure of lignin,

as shown in Fig. 7, with comparison to other widely used binders. The amphiphilic functional groups of LSS and thanks to its negative charged sulphonate group, the polysulphide dissolution can be efficiently blocked and it improves the ionic conductivity. The Li–S cell with the LSS binder shows the sustained capacity of  $\sim 661 \text{ mA h g}^{-1}$ .<sup>109</sup>

Thus, the inexpensive biomass-derived material has been used due to its variety of functional groups, which make it suitable for any role within Li-based batteries, particularly within Li–S batteries, where it can tackle the prime problem of the Li–S system by alleviation of the shuttle effect. We would like to address that besides Li–S as a next-generation battery system, and the exploiting of lignin in other Li-based systems has already been on the way. For example, lithium–oxygen ( $\text{Li}–\text{O}_2$ ) batteries have emerged as the most promising candidate within lithium-based batteries, where lignin has so far been used in the form of activated carbon as the cathode, where various activation methods have been used such as KOH,  $\text{H}_3\text{PO}_4$  and steam activation methods. Due to these activation methods, the samples exhibited a higher surface area (over  $1000 \text{ m}^2 \text{ g}^{-1}$ ) along with defective area and vast functional groups. A higher discharge capacity of  $2.8 \text{ mA h cm}^{-2}$  at  $0.02 \text{ mA cm}^{-2}$  was observed with lignin activated via  $\text{H}_3\text{PO}_4$  (LPAC) and steam (LSAC), where LPAC shows a capacity retention of 100% over 800 cycles. Meanwhile, lignin with KOH (LKAC) exhibited the highest discharge capacity of  $7.2 \text{ mA h cm}^{-2}$  with up to 300 cycles. The cathode based on lignin carbon activated by different methods shows promising results with the low-cost fabrication process for lithium– $\text{O}_2$  batteries.<sup>110</sup>

Another promising system is lithium–selenium (Li–Se) batteries, which can be an alternative to the Li–S batteries, by replacing the cathode from sulphur to selenium, which avoids the polysulphide shuttling problem and can contribute significantly to improved electrical conductivity ( $\text{Se} = \sim 10^{-5} \text{ S cm}^{-1}$ ) with better electrochemical performance.

Thus far, alkaline lignin-derived porous carbon (LPC) has been used to produce Se/LPC composites by melt diffusion technique at  $260^\circ\text{C}$  to achieve encapsulated selenium into porous carbonaceous frameworks. Se/LPC shows high specific surface area, large pore volume and good electron conductivity that allow a smooth electrochemical reversible reaction of selenium with Li. The SE/LPC electrode in the Li–Se cell shows a specific capacity of  $596 \text{ mA h g}^{-1}$  and at  $0.5\text{C}$  with a capacity retention of  $453 \text{ mA h g}^{-1}$  over 300 cycles (Fig. 8).<sup>111</sup>

The 3D lignin hierarchical porous carbon could take up the higher Se loading due to classified porous structures providing a capacity of  $450 \text{ mA h g}^{-1}$  at  $0.5\text{C}$  after 500 cycles with an advantage of prolonged cycling life in the carbonate electrolyte. Due to the complex porous structure, selenium loss during charge–discharge would be reduced.<sup>112</sup>

However, the Li–Se system still faces the shuttle effect, and to help avoiding the shuttling of polyselenide species in the electrolyte that further demolishes the electrochemical performance, bamboo-derived porous carbon (PBC) was used as a framework for the encapsulation of elemental selenium, and the framework contains abundant meso/micropores. The Se/PBC cathode in Li–Se batteries shows an improved capacity of

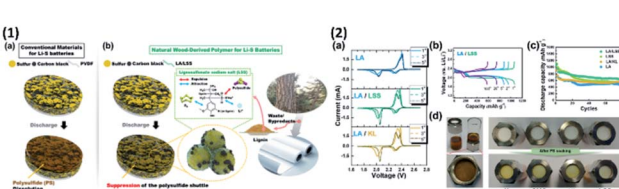


Fig. 7 (1) (a) Cathode with a conventional binder before and after discharge and (b) cathode with an LSS binder before and after discharge with the chemical structure of the LSS binder. (2) (a) CV curves of the Li–S cell with different binders like LA133 (LA), LA/lignosulphonate sodium salt (LA/LSS) and LA/kraft lignin (LA/KL) between the range of 1.7 and 2.7 V with  $0.1 \text{ mV s}^{-1}$  scan rate, (b) galvanostatic 1st, 2nd, 5th, 20th, and 100th cycle profiles at  $0.2\text{C}$  for LA/LSS, (c) cycling profile of the sulphur cathode with LA, LSS, LA/LSS, and LA/KL at  $0.2\text{C}$ , and (d) image of polysulphide reduction via a glass fiber filter-soaked pristine (x), CMC, KL and LSS solutions.<sup>109</sup>



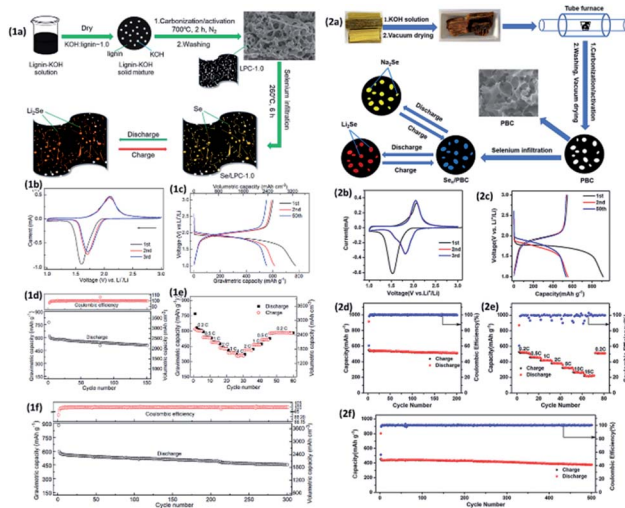


Fig. 8 (1a) Experimental scheme of preparation and application of selenium with lignin porous carbon (Se/LPC-1.0). (1b) CV curves at  $0.1 \text{ mV s}^{-1}$ . (1c) 1<sup>st</sup>, 2<sup>nd</sup> and 50<sup>th</sup> voltage profiles of Se/LPC-1.0 at 0.2C. (1d) Cycling performance of Se/LPC-1.0 at 0.2C. (1e) Rate capability profiles at different current densities. (1f) Galvanostatic cycling profile at 0.5C. (2a) Schematic of the experimental preparation process of Sen/PBC composites. (2b) CVs of Se50/PBC at  $0.1 \text{ mV s}^{-1}$  in the initial three cycles. (2c) Discharge-charge curves. (2d) Cycling performance of Se50/PBC at a current density of 0.2C. (2e) Rate performance and (2f) cycling performance at 0.5C of Se50/PBC for Li-Se batteries.<sup>113</sup>

509  $\text{mA h g}^{-1}$  within 200 cycles at C-rate of 0.2C, which proves that due to the 3D structure, porosity and huge surface area of PBC facilitate the transport of  $\text{Li}^+$  ions thanks to the buffering of the electrolyte volume change, leading to improved conductivity. Nevertheless, bamboo-derived porous carbon is a cheap and effective technique to avoid the shuttling and better performance of the Li-Se batteries.<sup>113</sup>

### 3. Conclusions

In this review, we tried to follow the possible advances of lignin as a material of choice in renewable lithium-based conventional and next-generation battery systems. Lignin has been explored by means of potential quinone functionality-related electrochemical properties, possible carbon source, its advantages and behaviour. The waste product extracted from the paper industry proves itself to be an interesting candidate for the high-performance energy storage systems, not only because it is cheaper and more abundant in nature than other well-known used materials but also because its impact globally are less harmful to completely extinct. However, the insulating nature of lignin still restricts mundane use of lignin in battery systems. Besides, the combination with a conductive synthetic polymer doesn't aid the idea of economic final product due to higher prices. Nevertheless, research done in the past decades has been substantial; despite, lignin and lignin-derived materials still face some challenges in the practical applications of the batteries. In addition, only limited lignin spin-off (i.e. kraft, lignosulphonate, and organosolv lignin) has been investigated. Thus, we believe that

the further investigation in this topic is rather crucial to fully understand and realise the replete properties and hidden occurrence of lignin for its commercialization.

In general, although there are still many challenges to overcome before lignin can be applied commercially in any energy storage system, great progress has been made in recent decades. Important advances have been attained to improve performance and understand the mechanism of the use of lignin-derived materials. We believe that forthcoming research investigation through the scientific community will open a path to much more interesting outcomes and ultimately will make lignin a highly valuable material towards practical industrial applications.

It is becoming much clearer with recent studies that lignin as a low-cost and environmentally friendly material can be capable of being a future of battery systems. However, achieving lignin-based renewable biobatteries will have a high impact on improving world's economy and will also promote a greener environment.

### Conflicts of interest

There are no conflicts to declare.

### References

- Z. Yang, J. Zhang, M. C. W. W. Kintner-Meyer, X. Lu, D. Choi, J. P. Lemmon and J. Liu, *Chem. Rev.*, 2011, **111**, 3577–3613.
- M. Armand and J.-M. Tarascon, *Nature*, 2008, **451**, 652–657.
- R. Holze, *J. Solid State Electrochem.*, 2015, **19**, 1253.
- N.-S. Choi, Z. Chen, S. A. Freunberger, X. Ji, Y.-K. Sun, K. Amine, G. Yushin, L. F. Nazar, J. Cho and P. G. Bruce, *Angew. Chem. Int. Ed.*, 2012, **51**, 9994–10024.
- J. B. Goodenough and Y. Kim, *Chem. Mater.*, 2010, **22**, 587–603.
- J. B. Goodenough and K.-S. Park, *J. Am. Chem. Soc.*, 2013, **135**, 1167–1176.
- Y. Liang, Z. Tao and J. Chen, *Adv. Energy Mater.*, 2012, **2**, 742–769.
- M. Miroshnikov, K. P. Divya, G. Babu, A. Meiyazhagan, L. M. Reddy Arava, P. M. Ajayan and G. John, *J. Mater. Chem. A*, 2016, **4**, 12370–12386.
- L. Zhang, Z. Liu, G. Cui and L. Chen, *Prog. Polym. Sci.*, 2014, **43**, 136–164.
- X. Wu, J. Jiang, C. Wang, J. Liu, Y. Pu, A. Ragauskas, S. Li and B. Yang, *Biofuels, Bioprod. Bioref.*, 2020, **14**, 650–672.
- J. Zhu, C. Yan, X. Zhang, C. Yang, M. Jiang and X. Zhang, *Prog. Energy Combust. Sci.*, 2020, **76**, 100788.
- T. C. Nirmale, B. B. Kale and A. J. Varma, *Int. J. Biol. Macromol.*, 2017, **103**, 1032–1043.
- D. Wang, S. H. Lee, J. Kim and C. B. Park, *ChemSusChem*, 2020, **13**, 2807–2827.
- J. L. Espinoza-Acosta, P. I. Torres-Chávez, J. L. Olmedo-Martínez, A. Vega-Ríos, S. Flores-Gallardo and E. A. Zaragoza-Contreras, *J. Energy Chem.*, 2018, **27**, 1422–1438.
- S. Mehta, S. Jha and H. Liang, *Renewable Sustainable Energy Rev.*, 2020, **134**, 110345.



16 K. R. Hakeem, J. Mohammad and O. Alothman, *Agricultural Biomass Based Potential Materials*, 2015.

17 S. V. Obydenkova, P. D. Kouris, E. J. M. M. Hensen, H. J. Heeres and M. D. Boot, *Bioresour. Technol.*, 2017, **243**, 589–599.

18 A. J. Ragauskas, G. T. Beckham, M. J. Biddy, R. Chandra, F. Chen, M. F. Davis, B. H. Davison, R. A. Dixon, P. Gilna, M. Keller, P. Langan, A. K. Naskar, J. N. Saddler, T. J. Tschaplinski, G. A. Tuskan and C. E. Wyman, *Science*, 2014, **344**, 709.

19 Q. Li, A. J. Ragauskas and J. S. Yuan, *Tappi J.*, 2017, **16**, 107–108.

20 J. Becker and C. Wittmann, *Biotechnol. Adv.*, 2019, **37**, 107360.

21 J. Zhu, C. Yan, X. Zhang, C. Yang, M. Jiang and X. Zhang, *Prog. Energy Combust. Sci.*, 2020, **76**, 100788.

22 E. I. Chupka and T. M. Rykova, *Chem. Nat. Compd.*, 1983, **19**, 78–80.

23 S. V. Gnedenkov, D. P. Opra, L. A. Zemnukhova, S. L. Sinebryukhov, I. A. Kedrinskii, O. V. Patrusheva and V. I. Sergienko, *J. Energy Chem.*, 2015, **24**, 346–352.

24 G. Torgovnikov, *Dielectric Properties of Wood and Wood-Based Materials*, 1993, vol. 1.

25 A. Naseem, S. Tabasum, K. M. Zia, M. Zuber, M. Ali and A. Noreen, *Int. J. Biol. Macromol.*, 2016, **93**, 296–313.

26 S. Laurichesse and L. Avérous, *Prog. Polym. Sci.*, 2014, **39**, 1266–1290.

27 V. K. Ponnusamy, D. D. Nguyen, J. Dharmaraja, S. Shobana, J. R. Banu, R. G. Saratale, S. W. Chang and G. Kumar, *Bioresour. Technol.*, 2019, **271**, 462–472.

28 M. N. Collins, M. Nechifor, F. Tanasă, M. Zănoagă, A. McLoughlin, M. A. Strózyk, M. Culebras and C. A. Teacă, *Int. J. Biol. Macromol.*, 2019, **131**, 828–849.

29 O. Y. Abdelaziz, D. P. Brink, J. Prothmann, K. Ravi, M. Sun, J. García-Hidalgo, M. Sandahl, C. P. Hulteberg, C. Turner, G. Lidén and M. F. Gorwa-Grauslund, *Biotechnol. Adv.*, 2016, **34**, 1318–1346.

30 P. Azadi, O. R. Inderwildi, R. Farnood and D. A. King, *Renewable Sustainable Energy Rev.*, 2013, **21**, 506–523.

31 J. Sameni, S. A. Jaffer, J. Tjong and M. Sain, *Curr. For. Rep.*, 2020, **6**, 159–171.

32 A. Kumar, Anushree, J. Kumar and T. Bhaskar, *J. Energy Inst.*, 2020, **93**, 235–271.

33 O. Yu and K. H. Kim, *Appl. Sci.*, 2020, **10**, 4626.

34 A. Romaní, H. A. Ruiz, J. A. Teixeira and L. Domingues, *Renewable Energy*, 2016, **95**, 1–9.

35 H. Shaghaleh, X. Xu and S. Wang, *RSC Adv.*, 2018, **8**, 825–842.

36 VTT TIEDOTTEITA – Research Notes 2558, ed. A. Harlin and M. Vikman, 2010.

37 B. Lee, Y. Ko, G. Kwon, S. Lee, K. Ku, J. Kim and K. Kang, *Joule*, 2018, **2**, 61–75.

38 E. J. Son, J. H. Kim, K. Kim and C. B. Park, *J. Mater. Chem. A*, 2016, **4**, 11179–11202.

39 G. Milczarek, *Langmuir*, 2009, **25**, 10345–10353.

40 G. Milczarek, *Electrochim. Acta*, 2009, **54**, 3199–3205.

41 G. Milczarek, *Electroanalysis*, 2008, **20**, 211–214.

42 F. N. Ajjan, M. Ambrogi, G. A. Tiruye, D. Cordella, A. M. Fernandes, K. Grygiel, M. Isik, N. Patil, L. Porcarelli, G. Rocasalbas, G. Vendrami, E. Zeglio, M. Antonietti, C. Detrembleur, O. Inganäs, C. Jérôme, R. Marcilla, D. Mecerreyes, M. Moreno, D. Taton, N. Solin and J. Yuan, *Polym. Int.*, 2017, **66**, 1119–1128.

43 S. Admassie, F. N. Ajjan, A. Elfwing and O. Inganäs, *Mater. Horiz.*, 2016, **3**, 174–185.

44 T. Rębiś, T. Y. Nilsson and O. Inganäs, *J. Mater. Chem. A*, 2016, **4**, 1931–1940.

45 J. Tian, Z. Liu, Z. Li, W. Wang and H. Zhang, *RSC Adv.*, 2017, **7**, 12089–12097.

46 L. Li, L. Huang, R. J. Linhardt, N. Koratkar and T. Simmons, *Sustainable Energy Fuels*, 2018, **2**, 422–429.

47 C. Lai, Z. Zhou, L. Zhang, X. Wang, Q. Zhou, Y. Zhao, Y. Wang, X. F. Wu, Z. Zhu and H. Fong, *J. Power Sources*, 2014, **247**, 134–141.

48 S. V. Gnedenkov, D. P. Opra, S. L. Sinebryukhov, A. K. Tsvetnikov, A. Y. Ustinov and V. I. Sergienko, *J. Ind. Eng. Chem.*, 2014, **20**, 903–910.

49 Z. Z. Chang, B. J. Yu and C. Y. Wang, *Electrochim. Acta*, 2015, **176**, 1352–1357.

50 M. Culebras, H. Geaney, A. Beaucamp, P. Upadhyaya, E. Dalton, K. M. Ryan and M. N. Collins, *ChemSusChem*, 2019, **12**, 4516–4521.

51 S. Chaleawlert-umpon, T. Berthold, X. Wang, M. Antonietti and C. Liedel, *Adv. Mater. Interfaces*, 2017, **4**, 1–7.

52 T. Chen, Q. Zhang, J. Pan, J. Xu, Y. Liu, M. Al-Shroofy and Y. T. Cheng, *ACS Appl. Mater. Interfaces*, 2016, **8**, 32341–32348.

53 D. I. Choi, J. N. Lee, J. Song, P. H. Kang, J. K. Park and Y. M. Lee, *J. Solid State Electrochem.*, 2013, **17**, 2471–2475.

54 T. Liu, S. Sun, W. Song, X. Sun, Q. Niu, H. Liu, T. Ohsaka and J. Wu, *J. Mater. Chem. A*, 2018, **6**, 23486–23494.

55 A. P. Nowak, J. Hagberg, S. Leijonmarck, H. Schweinebarth, D. Baker, A. Uhlin, P. Tomani and G. Lindbergh, *Holzforschung*, 2018, **72**, 81–90.

56 W. Chen, M. Luo, K. Yang and X. Zhou, *Microporous Mesoporous Mater.*, 2020, **300**, 110178.

57 P. Salehian, K. Karimi, H. Zilouei and A. Jeihanipour, *Fuel*, 2013, **106**, 484–489.

58 J. Xu, B. Liu, H. Hou and J. Hu, *Bioresour. Technol.*, 2017, **234**, 406–414.

59 O. Merino, V. Almazán, R. Martínez-Palou and J. Aburto, *Waste Biomass Valorization*, 2017, **8**, 733–742.

60 O. I. Grzegorz Milczarek, *Science*, 2012, **335**, 1468–1472.

61 M. Quan, D. Sanchez, M. F. Wasylkiw and D. K. Smith, *J. Am. Chem. Soc.*, 2007, **129**, 12847–12856.

62 H. Chen, M. Armand, M. Courty, M. Jiang, C. P. Grey, F. Dolhem, J. Tarascon, P. Poizot and J. Verne, *J. Am. Chem. Soc.*, 2009, **131**(25), 8984–8988.

63 T. A. Enache and A. M. Oliveira-Brett, *J. Electroanal. Chem.*, 2011, **655**, 9–16.

64 T. Grygar, Š. Kučková, D. Hradil and D. Hradilová, *J. Solid State Electrochem.*, 2003, **7**, 706–713.

65 D. Schmidt, M. D. Hager and U. S. Schubert, *Adv. Energy Mater.*, 2016, **6**, 1500369.



66 H. Wang, F. Li, B. Zhu, L. Guo, Y. Yang, R. Hao, H. Wang, Y. Liu, W. Wang, X. Guo and X. Chen, *Adv. Funct. Mater.*, 2016, **26**, 3472–3479.

67 P. Hu, H. Wang, Y. Yang, J. Yang, J. Lin and L. Guo, *Adv. Mater.*, 2016, **28**, 3486–3492.

68 K. Oyaizu, Y. Niibori, A. Takahashi and H. Nishide, *J. Inorg. Organomet. Polym. Mater.*, 2013, **23**, 243–250.

69 Y. Yang, H. Wang, R. Hao and L. Guo, *Small*, 2016, **12**, 4683–4689.

70 P. C. Rodrigues, P. Cant and M. A. B. Gomes, *Eur. Polym. J.*, 2002, **38**, 2213–2217.

71 Z. Zhu, M. Hong, D. Guo, J. Shi, Z. Tao and J. Chen, *J. Am. Chem. Soc.*, 2014, **136**, 16461–16464.

72 F. N. Ajjan, M. J. Jafari, T. Rebić, T. Ederth and O. Inganäs, *J. Mater. Chem. A*, 2015, **3**, 12927–12937.

73 M. Wagner, T. Rebić and O. Inganäs, *J. Power Sources*, 2016, **302**, 324–330.

74 P. K. Kulkarni, A. G. Satyanarayana and K. G. Rohatgi, *J. Mater. Sci. Lett.*, 1981, **16**, 1719–1726.

75 Y. Liang, P. Zhang and J. Chen, *Chem. Sci.*, 2013, **4**, 1330–1337.

76 J. Geng, J.-P. Bonnet, S. Renault, F. Dolhem and P. Poizot, *Energy Environ. Sci.*, 2010, **3**, 1929–1933.

77 S. Renault, J. Geng, F. Dolhem and P. Poizot, *Chem. Commun.*, 2011, **47**, 2414–2416.

78 W. Huang, Z. Zhu, L. Wang, S. Wang, H. Li, Z. Tao, J. Shi, L. Guan and J. Chen, *Angew. Chem. Int. Ed.*, 2013, **52**, 9162–9166.

79 B. Genorio, K. Pirnat, R. Cerc-Korosec, R. Dominko and M. Gaberscek, *Angew. Chem. Int. Ed.*, 2010, **49**, 7222–7224.

80 L. Zhang, Z. Liu, G. Cui and L. Chen, *Prog. Polym. Sci.*, 2015, **43**, 136–164.

81 G. Milczarek, *Electroanalysis*, 2007, **19**, 1411–1414.

82 C. A. S. Hill, *Wood Modif.*, 2006, vol. 1–18.

83 M. Matrakova, T. Rogachev, D. Pavlov and B. O. Myrvold, *J. Power Sources*, 2003, **113**, 345–354.

84 K. Xia, Q. Ouyang, Y. Chen, X. Wang, X. Qian and L. Wang, *ACS Sustain. Chem. Eng.*, 2016, **4**, 159–168.

85 W. E. Tenhaeff, O. Rios, K. More and M. A. McGuire, *Adv. Funct. Mater.*, 2014, **24**, 86–94.

86 H. Lu and X. S. Zhao, *Sustainable Energy Fuels*, 2017, **1**, 1265–1281.

87 A. Manuscript, S. Chaleawlert-Umporn and C. Liedel, *J. Mater. Chem. A*, 2017, **5**, 24344–24352.

88 S. Chatterjee, T. Saito, O. Rios and A. Johs, *ACS Symp. Ser.*, 2014, **1186**, 203–218.

89 S. Kubo and J. F. Kadla, *J. Polym. Environ.*, 2005, **13**, 97–105.

90 A. M. Navarro-Suárez, D. Saurel, P. Sánchez-Fontecoba, E. Castillo-Martínez, J. Carretero-González and T. Rojo, *J. Power Sources*, 2018, **397**, 296–306.

91 L. Zhang, T. You, T. Zhou, X. Zhou and F. Xu, *ACS Appl. Mater. Interfaces*, 2016, **8**, 13918–13925.

92 S. V. V. V. Gnedenkov, S. L. L. L. Sinebryukhov, D. P. P. P. Opra, L. A. A. A. Zemnukhova, A. K. K. Tsvetnikov, A. N. N. Minaev, A. A. A. Sokolov and V. I. I. Sergienko, *Procedia Chem.*, 2014, **11**, 96–100.

93 H. Qiao and Q. Wei, *Functional nanofibers in lithium-ion batteries*, Woodhead Publishing Limited, 2012.

94 A. M. Navarro-Suárez, J. Carretero-González, N. Casado, D. Mecerreyres, T. Rojo and E. Castillo-Martínez, *Sustainable Energy Fuels*, 2018, **2**, 836–842.

95 M. Zhu, J. Wu, B. Liu, W. H. Zhong, J. Lan, X. Yang and G. Sui, *J. Membr. Sci.*, 2019, **588**, 117194.

96 C. Y. Chou, J. R. Kuo and S. C. Yen, *ACS Sustain. Chem. Eng.*, 2018, **6**, 4759–4766.

97 L. Du, W. Wu, C. Luo, H. Zhao, D. Xu, R. Wang and Y. Deng, *Solid State Ionics*, 2018, **319**, 77–82.

98 Z. Zhou, F. Chen, T. Kuang, L. Chang, J. Yang, P. Fan, Z. Zhao and M. Zhong, *Electrochim. Acta*, 2018, **274**, 288–297.

99 Y. Ma, K. Chen, J. Ma, G. Xu, S. Dong, B. Chen, J. Li, Z. Chen, X. Zhou and G. Cui, *Energy Environ. Sci.*, 2019, **12**, 273–280.

100 C. Luo, L. Du, W. Wu, H. Xu, G. Zhang, S. Li, C. Wang, Z. Lu and Y. Deng, *ACS Sustain. Chem. Eng.*, 2018, **6**, 12621–12629.

101 B. Liu, Y. Huang, H. Cao, A. Song, Y. Lin, M. Wang and X. Li, *J. Solid State Electrochem.*, 2018, **22**, 807–816.

102 H. Lu, A. Cornell, F. Alvarado, M. Behm, S. Leijonmarck, J. Li, P. Tomani and G. Lindbergh, *Materials*, 2016, **9**, 1–17.

103 F. Yu, Y. Li, M. Jia, T. Nan, H. Zhang, S. Zhao and Q. Shen, *J. Alloys Compd.*, 2017, **709**, 677–685.

104 Y. H. Lai, Y. T. Kuo, B. Y. Lai, Y. C. Lee and H. Y. Chen, *Int. J. Energy Res.*, 2019, **43**, 5803–5811.

105 X. Wu, C. Luo, L. Du, Y. Xiao, S. Li, J. Wang, C. Wang and Y. Deng, *ACS Sustain. Chem. Eng.*, 2019, **7**, 8413–8418.

106 A. Song, Y. Huang, X. Zhong, H. Cao, B. Liu, Y. Lin, M. Wang and X. Li, *J. Membr. Sci.*, 2018, **556**, 203–213.

107 J. S. Yeon, S. H. Park, J. Suk, H. Lee and H. S. Park, *Chem. Eng. J.*, 2020, **382**, 122946.

108 Z. Zhang, S. Yi, Y. Wei, H. Bian, R. Wang, Y. Min, H. L. S. Batteries, Z. Zhang, S. Yi, Y. Wei, H. Bian and R. Wang, *Polymers*, 2019, **11**, 1946.

109 J. Jeon, J.-K. K. Yoo, S. Yim, K. Jeon, G. H. Lee, J. H. Yun, D. K. Kim and Y. S. Jung, *ACS Sustain. Chem. Eng.*, 2019, **7**, 17580–17586.

110 G. Zhang, Y. Yao, T. Zhao, M. Wang and R. Chen, *ACS Appl. Mater. Interfaces*, 2020, **12**, 16521–16530.

111 H. Zhang, D. Jia, Z. Yang, F. Yu, Y. Su, D. Wang and Q. Shen, *Carbon*, 2017, **122**, 547–555.

112 P. Lu, F. Liu, F. Zhou, J. Qin, H. Shi and Z. S. Wu, *J. Energy Chem.*, 2021, **55**, 476–483.

113 C. Ma, H. Wang, X. Zhao, X. Wang, Y. Miao, L. Cheng, C. Wang, L. Wang, H. Yue and D. Zhang, *Energy Technol.*, 2020, **8**, 1–8.

